Mass Transfer Characteristics of Ozonolysis in Microreactors and Advanced-Flow Reactors

María José Nieves-Remacha[1] and Klavs F. Jensen[2]*

[1]*Present address: The Dow Chemical Company, 2301 North Brazosport Blvd. Bldg. B-1603, Freeport TX 77541, USA*
[2]*Department of Chemical Engineering, Massachusetts Institute of Technology, Cambridge MA 02139, USA*

Received: 17 March 2015; accepted: 14 April 2015

Ozonolysis of alkenes in liquid phase is conducted from micro scales to milli scales using a multichannel microreactor, a Corning low-flow reactor (LFR), and a Corning advanced-flow reactor (AFR). For the mass transfer limited test case of ozonolysis of 1-decene, maximum conversions that depend on the ozone availability in the gas phase are achieved regardless of the operating conditions, proving an excellent mass transfer in all three reactors. Ozonolysis of Sudan Red 7B dye provides visualization of the completion of the reaction in the glass-made AFR and LFR. Overall mass transfer coefficients are estimated to be on the order of 1/s in both the LFR and AFR, increasing with both liquid and gas flow rates. These values are within the same range observed in microchannels and one order of magnitude larger than in other conventional contactors.

Keywords: mass transfer, ozonolysis, 1-decene, Sudan Red dye, microchannels, advanced flow reactors

1. Introduction

The ozonolysis reaction has been studied since 1855 [1], and it has been used for decades for water purification and in organic synthesis with direct application in fine chemicals and pharmaceutical industries [2,3]. Oxidations in the presence of ozone have several advantages over other conventional oxidants, such as permanganate, osmium tetraoxide, periodic acid, or peroxides. The ozonolysis reaction is an environmentally friendly alternative to catalyzed oxidation reactions requiring very low activation energies in the absence of catalysts. In addition, the byproduct produced in ozonolysis is oxygen. It is also a very efficient reaction from an atom efficiency viewpoint.

However, there are issues related to safety due to the low-molecular weight unstable intermediates (ozonides, peroxides) produced during the reaction that can lead to explosions and limit the applicability of ozonolysis at large scales. In addition, ozonolysis is a very exothermic reaction (>50 kcal/mol) that requires extreme conditions of heat management and is normally carried out at −78 °C [2–6]. These limitations can be overcome using microreactor technology. First, microreactors reduce the accumulation of intermediates mitigating the risk of explosion during ozonolysis [7]. In addition, microreactors provide very high heat transfer rates, therefore, increasing the rate of heat dissipation and reducing the need of extreme heat management conditions. Ozonolysis reactions can be thus performed at ambient conditions while achieving high conversions and selectivities, as shown by Wada et al. using a multichannel microreactor [8].

Other examples of ozonolysis reactions performed in microreactors include the reaction with acetic acid 1-vinyl-hexyl ester in a falling film microreactor designed by the Institut für Mikrotechnik Mainz (IMM, Germany) [9] and an ozonolysis reduction sequence to synthesize vitamin D analogs in a microplant [10]. The latter study considered five different microstructured devices for the ozonolysis step: falling film microreactors designed by IMM and mikroglas (Invenios Europe, Germany), a cyclone mixer made by mikroglas, and five- and one-channel mixers typical for liquid–liquid reactions. The cyclone mixer and five-channel mixer demonstrated better performance than the falling film approach [10]. The Ley group pioneered the concept of using a semipermeable Teflon–2400 tube (90 cm ∂ long and 0.6 mm I.D.) for ozonolysis of several substrates with yields from 57 to 95% for 1 h residence time [11]. Irfan et al. performed ozonolysis of several substrates in a commercial flow reactor (O-Cube, ThalesNano, Hungary) from 0 °C to ambient temperature and flow rates in the range 0.2–2.0 mL/min, achieving isolated yields of 72–90% [12]. Most recently, Roydhouse et al. demonstrated the use of Vapourtec technology coupled with an ozone generator to perform ozonolysis of complex organic substrates in flow, observing good conversion (49–99%) to the corresponding aldehydes and ketones using an in-flow quench of triphenylphosphine [13,14].

The throughput of ozonolysis in microreactors is often low, on the order of mg/min. Except for the falling film microreactor from IMM [9] that can operate at gas flow rates of 100 mL/min and liquid flow rates of 1–15 mL/min, microreactors work at low flow rates (gas flow rate of 20 mL/min in the O-Cube [12] and 10 mL/min in the multichannel microreactor of Wada et al. [8]) or need very long reaction times to provide 100% conversions [11]. The small throughput limits the applicability of microreaction technology to the laboratory scale. Here, we consider scale-up to the advanced-flow reactor (AFR) manufactured by Corning Inc. that operates at flow rates in the range 10–300 mL/min. Since the increase in throughput in the AFR is achieved by increasing the channel size (1 mm of minimum channel dimension) from the micron scale to the milli scale, questions arise regarding the mass transfer performance in this device. Previous mass transfer studies of the AFR with 1-butanol/water/succinic acid [15], carbon dioxide/water [16], hexane/water [17] systems have shown that the overall mass transfer coefficients are in the range 0.1–10/s, depending on the flow rates of each phase [16,17].

With ozone in the gas phase and the alkene substrate in the liquid phase, the overall reaction rate for the ozonolysis reaction may be determined by either the mass transfer process of ozone from the gas to the liquid phase, either the intrinsic kinetics, or a combination of both competing processes. Regarding the transport rates, mass transfer coefficients for gas–liquid have been measured in the multichannel microreactor [8] and the AFR [16], yielding values of 2.5 and 0.2–3/s (depending on the phase flow rates), respectively. These values are at least one order of magnitude larger than the typical value for conventional stirred vessels for the same power consumption. On the other hand,

* Author for correspondence: kfjensen@mit.edu

DOI: 10.1556/1846.2015.00010
© 2015 Akadémiai Kiadó

kinetic rate constants for the ozonolysis of olefins with terminal double bonds, such as 1-hexene, 1-octene, and 1-decene, are high and similar (~10^5/M/s) [4,8]. Thus, the ozonolysis reaction rate would be expected to be controlled by mass transfer even operating at very low reagent concentrations in the microreactor and AFR [16].

The objective of this study is to demonstrate that ozonolysis can be conducted using the AFR technology at ambient temperature with a good reactor performance for the test case of 1-decene ozonolysis. Three reactors are used for this purpose: (a) a multichannel microreactor with posts and 54 μL volume as designed by Wada et al. [8], (b) a low-flow reactor (LFR) of 0.45 mL volume, and (c) AFR of 8.7 mL volume. Both the LFR and the AFR follow similar reactor designs in the form of heart-shaped cells in series providing a convergent–divergent configuration, which helps increase the specific interfacial area to provide high overall mass transfer coefficients.

2. Results and Discussion

Ozonolysis reactions were performed in the experimental setup shown in Figure 1 according to the procedures described in the Experimental Methods section. Three different reactors were used (Figure 2):

(a) Multichannel microreactor: design used by Wada et al. [8] composed by 16 reaction channels with posts to enhance mass transfer. Its internal volume is 54 μL.
(b) Low-flow reactor (LFR): manufactured by Corning Inc. [18], the LFR has an internal volume of 0.45 mL. Each module is designed by five rows of heart-shaped cells in series, which creates continuous breakup and coalescence of bubbles, enhancing mass transfer rates by creating large specific interfacial areas. The LFR is designed to study reactions in the laboratory at small scales. Operating flow rates range from 1 mL/min to 10 mL/min.
(c) Advanced-flow reactor (AFR): similar to the LFR, the AFR has 51 heart-shaped cells in series, with two posts inside as opposed to the single post present in the LFR. The volume for the AFR is 8.7 mL and is operated with flow rates from 10 to 100 mL/min [18].

Specifics of the experimental reaction conditions conducted at ambient temperature and outlet atmospheric pressure for the three reactors using 1-decene as substrate are summarized in Table S1 in Supporting Information.

The multichannel microreactor can operate with large ratios of gas-to-liquid flow rates (Q_G/Q_L = 86–286), making it possible to have sufficient amounts of ozone to achieve full conversions for higher concentrations of reagent. The recommended flow rates for the LFR and AFR as suggested by Corning are 2 to 10 g/min and 30 to 175 g/min, respectively [19]. The maximum flow rate is limited by the pressure drop along the reactor and maximum operating pressure. The maximum temperature the Gen1 Advanced-Flow reactors stand is 200 °C, and maximum pressure varies from 2.5 to 18 bar, depending on the working temperature. These operating conditions mainly depend on the connecting pieces between AFR modules. New generations of the AFR may be able to work in a broader range of operating conditions. Herein, we have used lower flow rates for the liquid phase in order to have a larger ozone-to-alkene ratio and explore whether full conversions can be achieved at those conditions. For the largest concentration of reagent (0.28 M), conversions below 21% were achieved at liquid flow rates below the recommended values (0.35 and 0.58 mL/min). Since the ozone concentration is limited by the ozone generator and the liquid flow rate was already operating below the recommended values, the remaining parameter to change was the reagent concentration.

Conversions above 99% were achieved at 0.07 M 1-decene for liquid flow rates of 0.23–0.35 mL/min and gas flow rates above 10 mL/min in the LFR. Similar results were obtained for the AFR. Operating at the largest gas flow rates (100 mL/min) provided sufficient ozone for the lowest liquid flow rates (5 mL/min) and substrate concentrations (0.05 M).

High selectivity towards the aldehyde 1-nonanal was only observed when using triphenylphosphine as the reducing agent. In the case of triethylphosphite, formation of nonanoic acid also occurred. This result is in accordance with the results found by Roydhouse et al. [13]. The same behavior is observed for the ozonolysis of ethyl sorbate, as shown in Table S2 of Supporting Information. It was again possible to achieve large conversions for the same operating conditions already discussed.

The question that remains unknown is whether there are mass transfer limitations in the LFR and AFR that prevent achieving higher conversions. In order to elucidate this, the experimental conversion of reagent for 1-decene and ethyl sorbate has been plotted versus the molar ratio of ozone to alkene and are compared with the theoretical maximum conversion in Figure 3. As seen from the results, for practically all experiments, the maximum conversion is achieved regardless of the operating conditions used as long as there is ozone available to react. The deviations from the theoretical maximum conversion

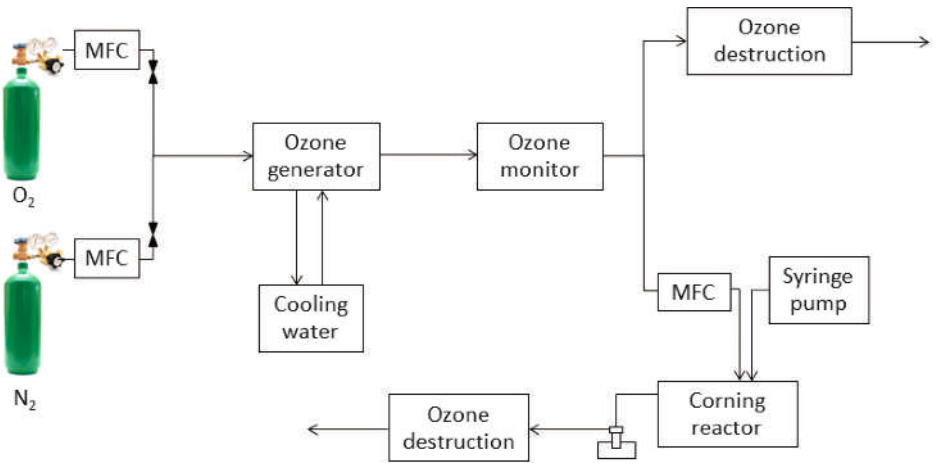

Figure 1. Experimental setup for ozonolysis. Oxygen and nitrogen stored in gas cylinders are introduced by mass flow controllers into the ozone generator. Ozone stream containing ~95% vol. O_2, ~5% vol. N_2, and ~5% vol. O_3 is introduced into the reactor using a mass flow controller. A syringe or peristaltic pump is used for liquid flow. The product is quenched with reducing agent at 0 °C in collecting vial

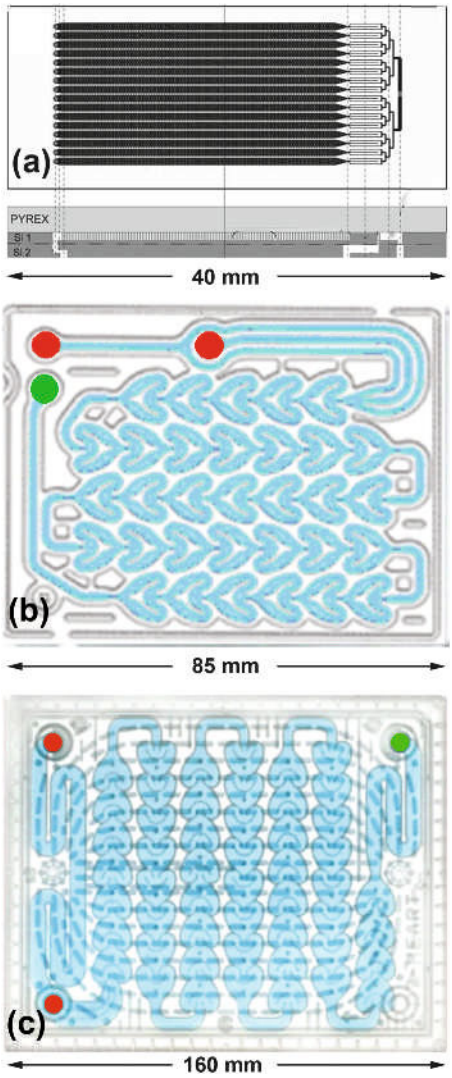

Figure 2. Reactors used in the ozonolysis experiments: (a) multichannel microreactor (volume = 0.054 mL) [8], (b) LFR (volume = 0.45 mL; height = 0.4 mm; minimum width = 0.4 mm) [18], and (c) AFR (volume = 8.7 mL; height = 1.1 mm; minimum width = 1 mm) [18]. In (b) and (c), red designates inlet and green represents outlet

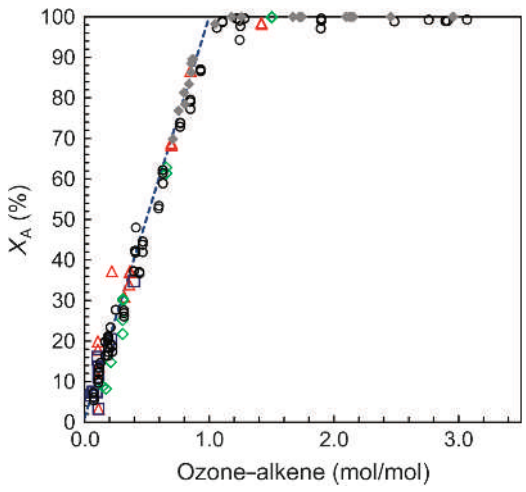

Figure 3. Alkene conversion (%) versus molar ratio ozone/alkene. Legend: ◆: multichannel microreactor; ◇: 1-decene in AFR; ○: 1-decene in LFR; △: ethylsorbate in AFR; □: ethylsorbate in LFR; - - -: theoretical maximum conversion. All reactors provide excellent mass transfer, which helps achieve maximum conversion estimated from the availability of ozone in the gas phase

are attributed to the associated experimental error and possible slight variations in the ozone concentration while the experiment was conducted. Since it was not possible to determine when the reaction was completed from these results, additional experiments were performed using Sudan Red 7B dye in the LFR and AFR.

A separate set of experiments involved the reaction of Sudan Red 7B dye, which allowed to monitor the conversion along the flow path of the reactor visually after the dye bleached. A concentration of 1 mM was used as comparison with the experiments conducted by O'Brian in a semipermeable Teflon AF-2400 [11]. The disappearance of red color upon oxidation by ozone determined the location where the reaction with substrate was completed. Instead of measuring substrate concentrations by gas chromatography, images of the reactor were recorded at different operating conditions. There was no need to calibrate the camera settings.

The resulting images are shown in Figures 4 and 5 for the AFR at constant gas flow rate and for the LFR at constant liquid flow rate, respectively. As it is seen from the images, the reactor length at which complete conversion is achieved increases with the liquid flow rate at a fixed ozone concentration and flow rate. At all flow rates, complete conversion is achieved within the first row of the AFR. For 1.5 mL/min of liquid flow rate in the LFR, complete conversions are reached even at the lowest gas flow rates in three heart cells.

Both the AFR and LFR were placed horizontally in order to eliminate gravity effects. The image shows only one instant of the flow. An alternating behavior was observed in the experiments, with bubbles passing through the top and bottom of the heart-cell alternatively. This is not observed at larger flow rates of gas in the LFR because most part of the gas occupies the heart cell in the form of a long bubble, whereas at the lower gas flow rates, there is an alternating flow of individual bubbles of gas through the top and bottom of the heart cell. This effect was also observed in computational fluid dynamic (CFD) simulations that were performed for two-phase flow in an AFR at the lowest flow rates, which may be due to the nonsymmetric entrance region of the reactor (Supporting Information, Figure S7).

The results of O'Brian et al. showed that 2.34 min was required for complete conversion of Sudan Red 7B dye (1 mM) in their semipermeable Teflon tube of 0.6 mm I.D. and 3-cm long. Here, in 0.5–0.6 s (depending on the liquid flow rate), complete conversion of the substrate is achieved. Bleaching of the red dye is observed at different positions depending on the liquid flow rate: for 5 mL/min, complete decoloration is observed at 1.5 hearts; for 10 mL/min, at the third heart; and for 20 mL/min, at the fifth heart. With a reactor model, the visualization experiments allow us to estimate the mass transfer coefficients in the two flow reactors. The reactor model assumes plug flow based on residence time distribution information obtained for single-phase and liquid–liquid flow (see Supporting Information). The deviation from plug flow is larger at the lowest flow rates. The reactor is composed by 51 heart cells, in which the presence of obstacles creates a continuous breakup and coalescence of bubbles which increase the mixing. The model includes mass transfer of ozone between gas and liquid phases, and reaction in the liquid phase between the substrate and the dissolved ozone. It is a simplified model that allows us to have an estimated value of overall mass transfer coefficients and observe trends when varying the liquid and gas flow rates. The governing equations are as follows:

$$\frac{\partial C_{O3}^{G}}{\partial z} = -\frac{k_L a}{U_G}\left(\mathrm{He}C_{O3}^{G} - C_{O3}^{L}\right) \quad (1)$$

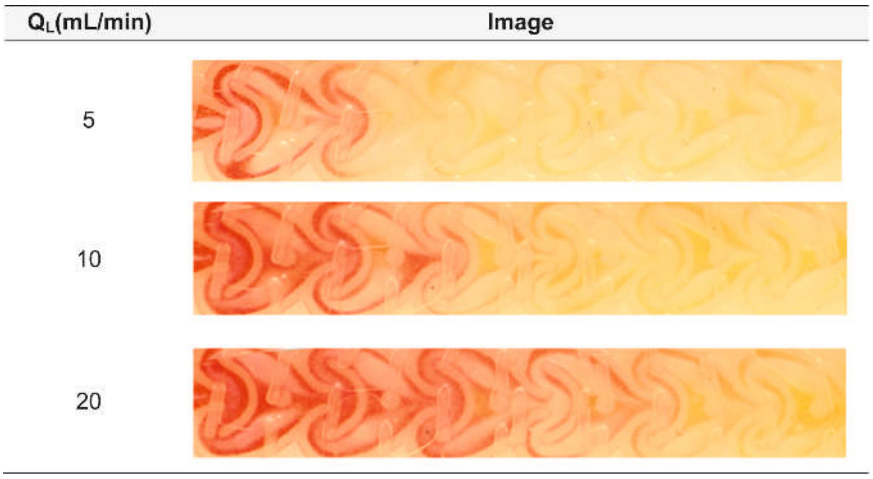

Figure 4. Images for ozonolysis of Sudan Red 7B dye (1 mM) in AFR with 100 mL/min gas flow rate. The excellent mass transfer rates in the AFR help achieve complete conversion within 1.5, 3, and 5 heart cells for 5, 10, and 20 mL/min liquid flow rate, respectively

$$\frac{\partial C_{O3}^{L}}{\partial z} = \frac{1}{U_L}\left(k_L a\left(\mathrm{He}C_{O3}^{G} - C_{O3}^{L}\right) - kC_i^L C_{O3}^L\right) \quad (2)$$

$$\frac{\partial C_i^L}{\partial z} = -\frac{1}{U_L} kC_i^L C_{O3}^L \quad (3)$$

Here, C_{O3}^{G} and C_{O3}^{L} are the ozone concentrations in the gas and liquid phases, respectively; C_i^L represents the alkene concentration in the liquid phase, and He is Henry's constant [20]; k is the kinetic rate constant and $k_L a$ designates the overall mass transfer coefficient (1/s); U_G and U_L are the gas and velocities, respectively; and z is the position along reactor path length (m).

The system of differential equations was solved using Matlab ordinary differential equation (ODE) solver for each experiment. The solver integrates the three differential equations simultaneously from $z = 0$ towards the end, given the flow rate of each phase, Henry constant for ozone, and initial concentration of substrate. Using the model to predict the observed conversions at the end of the first heart mixer allows estimation of the mass transfer coefficients, which vary with flow rates. In the AFR, the gas flow rate was fixed to 100 mL/min, whereas the liquid flow rates varied from 5 to 20 mL/min depending on the experiment. In the LFR, the liquid flow rate was fixed to 1.5 mL/min, whereas the gas flow rate increased from 4 to 10 mL/min. The resulting values for $k_L a$ are also expected to be different for each gas flow rate, being larger for larger gas flow rates.

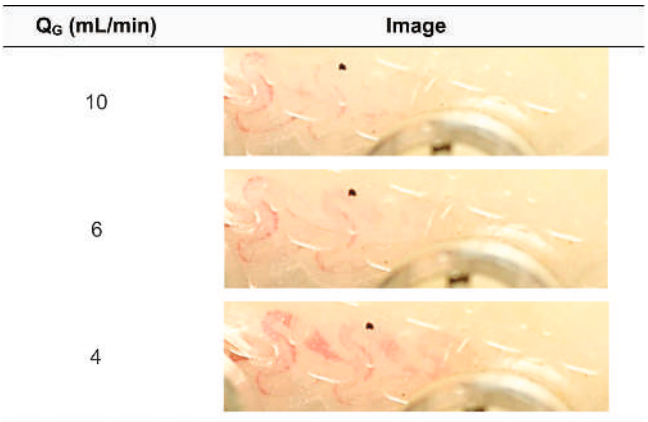

Figure 5. Images for ozonolysis of Sudan Red 7B dye (1 mM) in LFR at 1.5 mL/min and 10% wt. ozone in the gas phase. Excellent mass transfer rates are also achieved in the LFR. Complete conversions are obtained within the first three hearts for all gas flow rates

Experimental conversions are estimated based on the visualization experiments: (1) for 5 mL/min, the fraction converted is "1 heart/1.5 hearts," corresponding to 66% of the reagent; (2) for 10 mL/min, the fraction is "1 heart/3 hearts" corresponding to 33% conversion; and (3) for 20 mL/min, the fraction converted is "1 heart/5 hearts," corresponding to 20% conversion.

The model assumes linear variation of conversion along the reactor. For the calculation of the phase velocities, it was considered that the main stream splits into two streams of equal flow rates after encountering the first obstacle within the heart cell (supported by CFD simulations as shown by Figure S8 in Supporting Information where velocity profiles for single-phase and two-phase flows are included). The traveling distance of the fluid is essentially a result of the flow splitting into two streams after encountering the first post within the reactor, traveling at a speed which is approximately half the maximum speed encountered at the inlet of each heart-cell. It should be noted though that this is a simplification. More accurate results would be obtained if computational fluid dynamic simulations were performed to account for the spatial variations of velocities within the heart-cell. The model also assumes that the effect of consumption of ozone in the volumetric gas flow rate is negligible, since ozone is diluted in nitrogen. If pure ozone was used, a model incorporating volume change in the gas phase should be implemented. Values for $k_L a$ equal to 0.80, 0.86, and 0.96/s for the flow rates tested lead to conversions of 66%, 34%, and 20% in the AFR. For the LFR, the estimated overall mass transfer coefficients at constant liquid flow rate of 1.5 mL/min and decreasing gas flow rates (10, 6, and 4 mL/min) were 2.2, 1.7, and 1.4/s, respectively. The intrinsic kinetic constants for alkenes are on the order of 10^5–10^6 L/(mol s) [4,8]. For a range of concentrations between 1 mM and 0.1 M, the kinetic rates for the ozonolysis reaction are within the range 100–10,000/s. The overall mass transfer coefficients (/s) within microreactors and the advanced-flow reactors are of the order of 1/s, so the system is operating under mass transfer limited conditions.

The resulting overall mass transfer coefficients for the AFR and LFR are represented versus the residence time in Figure 6 and are compared with carbon dioxide–water system for horizontal and vertical orientation of the AFR module [16]. It is observed that for shorter residence times, the $k_L a$ values are on the order of 1/s and they decrease to 0.1/s for the longest residence times. For this reason, it is recommended to operate at large flow rates to ensure high mass transfer coefficients and, thus, enhanced reaction rates. These results are in agreement

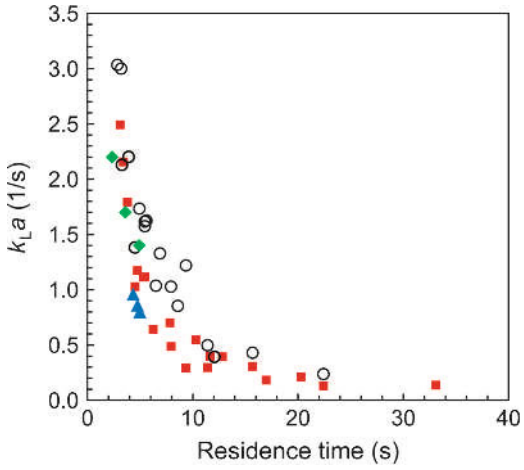

Figure 6. Overall mass transfer coefficients versus residence time. Legend: ■: CO_2/water AFR horizontal orientation; ○: CO_2/water AFR vertical orientation; ▲: Ozone/ethylacetate+alkene, AFR horizontal orientation; ◆: Ozone/ethylacetate+alkene, LFR horizontal orientation

with the observations from Woitalka et al. [15] for liquid–liquid systems, and are at least one order of magnitude larger if compared to conventional multiphase contactors [16,17].

The slightly lower k_La values obtained for the ozone/ethylacetate–alkene system compared to the CO_2–water case are consistent with the lower solubility of ozone [20] (additional details in Supporting Information). Good agreement is observed between experimental conversions and model predictions using the estimated mass transfer coefficients for ozone–Sudan Red dye for the ozonolysis of 1-decene as shown by Figure 7.

3. Conclusions

Ozonolysis of alkenes has been conducted in a multichannel microreactor, a low-flow reactor (LFR), and an advanced-flow reactor (AFR) to determine mass transfer performance in ozonolysis in flow reactors from micro to milli scales. For this reaction, the kinetic rate constants are high (~10^5/M/s [4,8]), so the limiting step is the mass transfer process of ozone from the gas to the liquid phase. The maximum conversion of alkene achievable from the amount of ozone available in the gas phase was realized in all reactors, regardless of the operating conditions tested. Ozonolysis of Sudan Red 7B dye in the AFR and the LFR showed that the reaction was completed within the first row of hearts in both reactors. Values for k_La were estimated for the AFR and LFR, being on the order of 1/s, and increasing with both liquid and gas flow rates. These are of the same order of magnitude as microreactors and at least one order of magnitude larger than other conventional contactors. These results are in agreement with the findings of Woitalka et al., who studied the scalability of mass transfer in liquid–liquid systems [15]. The higher flow rates in the AFR help increase production versus the use of microreactors while still achieving high mass transfer rates, enabling multiphase reactions that would otherwise suffer from mass transfer limitations in conventional contactors.

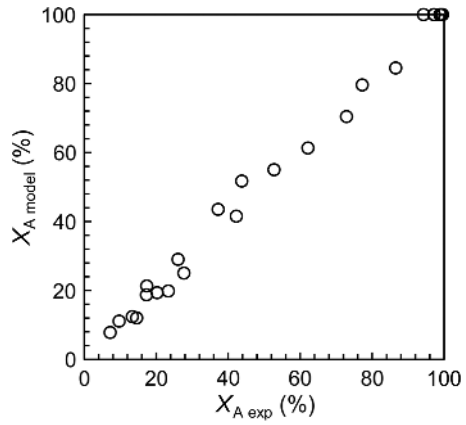

Figure 7. Predicted and experimental conversion of alkene

Regarding the operating parameters of each reactor, the multichannel microreactor operates at flow rate ratios of gas–liquid that can range from 90 to 290 ensuring enough ozone availability. However, the LFR and AFR work at approximate ratios of 10–60 for the recommended flow rates (10 mL/min and 100 mL/min, respectively), which limits the application of these reactors at higher substrate concentrations and ozone concentrations of 10% weight if reaction occurs in a single pass. Recycling of the product after separation of the gas stream or working with higher ozone concentrations would address this issue.

On the other hand, the multichannel microreactor with a volume of 54 μL provides a very low throughput, whereas the LFR and AFR operate at larger scales: one or two orders of magnitude larger, respectively, in comparison with the microreactor. In addition, several modules in parallel could be easily mounted to scale-out the reaction and achieve even larger production rates.

4. Experimental

4.1. Materials. Chemicals were used as received without prior purification steps. Potassium iodide, 1-decene, ethyl sorbate, triethylphosphite, and triphenylphosphine were purchased from Alfa Aesar, ethylacetate (solvent) from VWR, and the internal standard tridecane and Sudan Red 7B dye, from Sigma-Aldrich. 1-Decene and ethyl sorbate were used as substrates for the ozonolysis reaction with concentrations ranging from 0.05 M to 0.28 M, while tridecane was used as internal standard due to its slow oxidation rate with ozone [8]. Triethylphosphite and triphenylphosphine 0.28 M in ethyl acetate solutions were used as quench agents [8,14]. Nitrogen and oxygen gas cylinders were purchased from Airgas.

4.2. Experimental Setup. The experimental setup for the ozonolysis study is shown in Figure 1. Ozone was produced in a water cooled ozone generator OT-5 from Ozone Technology AB. The inlet composition of the ozone generator was 95% volume oxygen and 5% volume nitrogen, as recommended for maximum ozone production. The nitrogen and oxygen flow rates to the ozone generator were delivered using precalibrated mass flow controllers (UNIT). The ozone concentration was measured inline right at the outlet of the ozone generator using an ozone monitor (Teledyne Instruments Model 454H). Concentrations ranged from 4 to 13% weight, depending on inlet pressure, temperatures, humidity, and flow rates. A mass flow controller (Aalborg) delivered the ozone–oxygen–nitrogen mixture to the reactor.

The reagent solution was delivered to the microreactor and the low-flow reactor (LFR) using a syringe pump (Harvard Apparatus PHD2000) and to the AFR using a peristaltic pump (Thermo Scientific). Experiments were conducted at ambient temperature and atmospheric pressure at the outlet of the reactor. Samples of the liquid phase were collected at steady-state in glass vials containing the quench solution at 0 °C to prevent evaporation and were analyzed through gas chromatography. Unreacted ozone at the outlet of the reactor and the waste stream from the ozone generator were destroyed by bubbling the gas stream through an aqueous solution of potassium iodide 5% wt.

Ozonolysis experiments in the multichannel microreactor were performed using gas flow rates ranging from 5 to 10 sccm

and liquid flow rates from 0.116 to 0.035 mL/min. While the gas flow rate in the LFR was varied from 5 to 10 sccm, the liquid flow rate varied from 0.25 to 2 mL/min. The experiments performed in the AFR were conducted with gas flow rates of 100 sccm and liquid flow rates varying from 5 to 20 mL/min.

In addition, taking advantage of the transparency of the LFR and AFR glass reactors, experiments with Sudan Red 7B dye (1 mM) in ethyl acetate were performed to observe visually the progress of reaction. The original red color of this dye disappears after being oxidized by ozone, as already demonstrated by O'Brien et al. [11]. Thus, this experiment was used to determine at which point along the reactor flow path the ozonolysis reaction had been completed. Instead of measuring substrate concentrations using gas chromatography, images of the reactor were collected at different operating conditions.

Supporting Information

Electronic Supplementary Material is available in the online version at doi: 10.1556/1846.2015.00010.

Acknowledgments. We would like to acknowledge Novartis–MIT Center for Continuous Manufacturing for financial support and Corning Inc. for the low-flow and advanced-flow reactors.

References

1. Schönbein, C. F. *J. Prakt. Chem.* **1855**, *66*, 282.
2. Van Ornum, S. G.; Champeau, R. M.; Pariza, R. *Chem. Rev.* **2006**, *106*, 2990–3001.
3. Caron, S.; Dugger, R. W.; Ruggeri, S. G. Ragan, J. A.; Ripin, D. H. B. *Chem. Rev.* **2006**, *106*, 2943–2989.
4. Zaikov, G.; Rakovsky, S. *Ozonization of Organic and Polymer Compounds*; Smithers Rapra: Shawbury, 2009.
5. Deslongchamps, P.; Moreau, C. *Can. J. Chem.* **1971**, 49, 2465.
6. Criegee, R. *Angew. Chem. Int. Ed.* **1975**, *14*, 11.
7. Steinfeldt, N.; Bentrup, U.; Jähnisch, K. *Ind. Eng. Chem. Res.* **2010**, *49*, 72–80.
8. Wada, Y.; Schmidt, M. A.; Jensen, K. F. *Ind. Eng. Chem. Res.* **2006**, *45*, 8036–8042.
9. Steinfeldt, N.; Abdallah, R.; Dingerdissen, U.; Jähnisch, K. *Org. Process Res. Dev.* **2007**, *11*, 1025–1031.
10. Hübner, S.; Bentrup, U.; Budde, U.; Lovis, K.; Dietrich, T.; Freitag, A.; Küpper, L.; Jähnisch, K. *Org. Process Res. Dev.* **2009**, *13*, 952–960.
11. O'Brien, M.; Baxendale, I. R. Ley, S. V. *Org. Lett.* **2010**, *12*, 1596–1598.
12. Irfan, M.; Glasnov, T. N.; Kappe, C. O. *Org. Lett.* **2011**, *13*, 984–987.
13. Roydhouse, M. D.; Ghaini, A.; Constantinou, A. Cantu-Perez, A.; Motherwell, W. B.; Gavriilidis, A. *Org. Process Res. Dev.* **2011**, *15*, 989–996.
14. Roydhouse, M. D.; Motherwell, W. B.; Constantinou, A.; Gavriilidis, A.; Wheeler, R.; Down, K.; Campbell, I. *RSC Adv.* **2013**, *3*, 5076.
15. Woitalka, A.; Kuhn, S.; Jensen, K. F. *Chem. Eng. Sci.* **2014**, *116*, 1–8.
16. Nieves-Remacha, M. J.; Kulkarni, A. A.; Jensen, K. F. *Ind. Eng. Chem. Res.* **2013**, *52*, 8996–9010.
17. Nieves-Remacha, M. J.; Kulkarni, A. A.; Jensen, K. F. *Ind. Eng. Chem. Res.* **2012**, *51*, 16251–16262.
18. Corning Inc. Advanced-flow reactors website. http://www.corning.com/products_services/afr/index.aspx (accessed April 12, 2015).
19. Lavric, D. Advance Flow Reactors for Intensifying Two-Phase Process. Corning S.A.S.; France. Autumm Session PIN-NL 2014. http://www.traxxys.com/Symposia%20and%20PINNL%20sessions.html (accessed May 20, 2015).
20. Razumovskii, S. D.; Zaikov, G. E. *Bull. Acad. Sci. USSR, Div. Chem. Sci.*, **1971**, *20*, 616–620.